
Advances in Solid Oxide Fuel Cells II

*A Collection of Papers Presented at the
30th International Conference on
Advanced Ceramics and Composites
January 22–27, 2006,
Cocoa Beach, Florida*

Editor

Narottam P. Bansal

General Editors

Andrew Wereszczak

Edgar Lara-Curzio



A JOHN WILEY & SONS, INC., PUBLICATION

Advances in Solid Oxide Fuel Cells II

Advances in Solid Oxide Fuel Cells II

*A Collection of Papers Presented at the
30th International Conference on
Advanced Ceramics and Composites
January 22–27, 2006,
Cocoa Beach, Florida*

Editor

Narottam P. Bansal

General Editors

Andrew Wereszczak

Edgar Lara-Curzio



A JOHN WILEY & SONS, INC., PUBLICATION

Copyright © 2007 by the American Ceramics Society. All rights reserved.

Published by John Wiley & Sons, Inc., Hoboken, New Jersey
Published simultaneously in Canada.

No part of this publication may be reproduced, stored in a retrieval system or transmitted in any form or by any means, electronic, mechanical, photocopying, recording, scanning or otherwise, except as permitted under Section 107 or 108 of the 1976 United States Copyright Act, without either the prior written permission of the Publisher, or authorization through payment of the appropriate per-copy fee to the Copyright Clearance Center, Inc., 222 Rosewood Drive, Danvers, MA 01923, 978-750-8400, fax 978-646-8600, or on the web at www.copyright.com. Requests to the Publisher for permission should be addressed to the Permissions Department, John Wiley & Sons, Inc., 111 River Street, Hoboken, NJ 07030, (201) 748-6011, fax (201) 748-6008.

Limit of Liability/Disclaimer of Warranty: While the publisher and author have used their best efforts in preparing this book, they make no representation or warranties with respect to the accuracy or completeness of the contents of this book and specifically disclaim any implied warranties of merchantability or fitness for a particular purpose. No warranty may be created or extended by sales representatives or written sales materials. The advice and strategies contained herein may not be suitable for your situation. You should consult with a professional where appropriate. Neither the publisher nor author shall be liable for any loss of profit or any other commercial damages, including but not limited to special, incidental, consequential, or other damages.

For general information on our other products and services please contact our Customer Care Department within the U.S. at 877-762-2974, outside the U.S. at 317-572-3993 or fax 317-572-4002.

Wiley also publishes its books in a variety of electronic formats. Some content that appears in print, however, may not be available in electronic format.

Library of Congress Cataloging-in-Publication Data is available.

ISBN-13 978-0-470-08054-2
ISBN-10 0-470-08054-X

Printed in the United States of America.

1 0 9 8 7 6 5 4 3 2 1

Contents

Preface	xi
Introduction	xiii
Overview and Current Status	
Development of Two Types of Tubular SOFCs at TOTO	3
Akira Kawakami, Satoshi Matsuoka, Naoki Watanabe, Takeshi Saito, Akira Ueno, Tatsumi Ishihara, Natsuko Sakai, and Harumi Yokokawa	
Cell and Stack Development	
Development of Solid Oxide Fuel Cell Stack Using Lanthanum Gallate-Based Oxide as an Electrolyte	17
T. Yamada, N. Chitose, H. Etou, M. Yamada, K. Hosoi, N. Komada, T. Inagaki, F. Nishiwaki, K. Hashino, H. Yoshida, M. Kawano, S. Yamasaki, and T. Ishihara	
Anode Supported LSCM-LSGM-LSM Solid Oxide Fuel Cell	27
Alidad Mohammadi, Nigel M. Sammes, Jakub Pusz, and Alevtina L. Smirnova	
Characterization/Testing	
Influence of Anode Thickness on the Electrochemical Performance of Single Chamber Solid Oxide Fuel Cells	37
B. E. Buegler, Y. Santschi, M. Felberbaum, and L. J. Gauckler	
Investigation of Performance Degradation of SOFC Using Chromium-Containing Alloy Interconnects	47
D. R. Beeaff, A. Dinesen, and P. V. Hendriksen	
Degradation Mechanism of Metal Supported Atmospheric Plasma Sprayed Solid Oxide Fuel Cells	55
D. Hathiramani, R. Vaßen, J. Mertens, D. Sebold, V. A. C. Haanappel, and D. Stover	

Effect of Transition Metal Ions on the Conductivity and Stability of Stabilized Zirconia D. Lybye and M. Mogensen	67
Thermophysical Properties of YSZ and Ni-YSZ as a Function of Temperature and Porosity M. Radovic, E. Lara-Curzio, R. M. Trejo, H. Wang, and W. D. Porter	79
Physical Properties in the $\text{Bi}_2\text{O}_3\text{-Fe}_2\text{O}_3$ System Containing Y_2O_3 and CaO Dopants Hsin-Chai Huang, Yu-Chen Chang, and Tzer-Shin Sheu	87
Electrical Properties of $\text{Ce}_{0.8}\text{Gd}_{0.2}\text{O}_{1.9}$ Ceramics Prepared by an Aqueous Process Toshiaki Yamaguchi, Yasufumi Suzuki, Wataru Sakamoto, and Shin-ichi Hirano	95
Structural Study and Conductivity of $\text{BaZr}_{0.90}\text{Ga}_{0.10}\text{O}_{2.95}$ Istaq Ahmed, Elisabet Ahlberg, Sten Eriksson, Christopher Knee, Maths Karlsson, Aleksandar Matic, and Lars Borjesson	105
Hydrogen Flux in Terbium Doped Strontium Cerate Membrane Mohamed M. Elbaccouch and Ali T-Raissi	119
A Mechanical-Electrochemical Theory of Defects in Ionic Solids Narasimhan Swaminathan and Jianmin Qu	125
 Electrodes	
Nanostructured Ceramic Suspensions for Electrodes and the Brazilian SOFC Network "Rede PaCOS" R. C. Cordeiro, G. S. Trindade, R. N. S. H. Magalhães, G. C. Silva, P. R. Villalobos, M. C. R. S. Varela, and P. E. V. de Miranda	139
Modeling of MIEC Cathodes: The Effect of Sheet Resistance David S. Mebane, Erik Koep, and Meilin Liu	153
Cathode Thermal Delamination Study for a Planar Solid Oxide Fuel Cell with Functional Graded Properties: Experimental Investigation and Numerical Results Gang Ju, Kenneth Reifsnider, and Jeong-Ho Kim	161
Electrochemical Characteristics of Ni/Gd-Doped Ceria and Ni/Sm-Doped Ceria Anodes for SOFC Using Dry Methane Fuel Caroline Levy, Shinichi Hasegawa, Shiko Nakamura, Manabu Ihara, and Keiji Yamahara	175

Control of Microstructure of NiO-SDC Composite Particles for Development of High Performance SOFC Anodes 183
Koichi Kawahara, Seiichi Suda, Seiji Takahashi, Mitsunobu Kawano, Hiroyuki Yoshida, and Toru Inagaki

Electrochemical Characterization and Identification of Reaction Sites in Oxide Anodes 193
T. Nakamura, K. Yashiro, A. Kairnai, T. Otake, K. Sato, G.J. Park, T. Kawada, and J. Mizusaki

Interconnects and Protective Coatings

Corrosion Performance of Ferritic Steel for SOFC Interconnect Applications 201
M. Ziomek-Moroz, G. R. Holcomb, B. S. Covino, Jr., S. J. Bullard, P. D. Jablonski, and D. E. Alman

High Temperature Corrosion Behavior of Oxidation Resistant Alloys Under SOFC Interconnect Dual Exposures 211
Zhenguo Yang, Greg W. Coffey, Joseph P. Rice, Prabhakar Singh, Jeffrey W. Stevenson, and Guan-Guang Xia

Electro-Deposited Protective Coatings for Planar Solid Oxide Fuel Cell Interconnects 223
Christopher Johnson, Chad Schaeffer, Heidi Barron, and Randall Gemmen

Properties of $(\text{Mn}, \text{Co})_3\text{O}_4$ Spinel Protection Layers for SOFC Interconnects 231
Zhenguo Yang, Xiao-Hong Li, Gary D. Maupin, Prabhakar Singh, Steve P. Sirmner, Jeffrey W. Stevenson, Guan-Guang Xia, and Xiaodong Zhou

Fuel Cell Interconnecting Coatings Produced by Different Thermal Spray Techniques 241
E. Garcia and T. W. Coyle

Surface Modification of Alloys for Improved Oxidation Resistance in SOFC Applications 253
David E. Alman, Paul D. Jablonski, and Steven C. Kung

Seals

Composite Seal Development and Evaluation 265
Matthew M. Seabaugh, Kathy Sabolsky, Gene B. Arkenberg, and Jerry L. Jayjohn

Investigation of SOFC-Gaskets Containing Compressive Mica Layers Under Dual Atmosphere Conditions 273
F. Wiener, M. Bram, H.-P. Buchkremer, and D. Sebold

Performance of Self-Healing Seals for Solid Oxide Fuel Cells (SOFC)	287
Raj N. Singh and Shailendra S. Parihar	
Properties of Glass-Ceramic for Solid Oxide Fuel Cells	297
S. T. Reis, R. K. Brow, T. Zhang, and P. Jasinski	
Mechanical Behavior of Solid Oxide Fuel Cell (SOFC) Seal Glass-Boron Nitride Nanotubes Composite	305
Sung R. Choi, Narottam P. Bansal, Janet B. Hurst, and Anita Garg	
Mechanical Behaviour of Glassy Composite Seals for IT-SOFC Application	315
K. A. Nielsen, M. Solvang, S. B. L. Nielsen, and D. Beeaff	
Mechanical Property Characterizations and Performance Modeling of SOFC Seals	325
Brian J. Koeppel, John S. Vetrano, Ba Nghiep Nguyen, Xin Sun, and Moe A. Khaleel	
 Mechanical Properties	
Fracture Test of Thin Sheet Electrolytes	339
Jurgen Malzbender, Rolf W. Steinbrech, and Lorenz Singheiser	
Failure Modes of Thin Supported Membranes	347
P. V. Hendriksen, J. R. Høgsberg, A. M. Kjeldsen, B. F. Sørensen, and H. G. Pedersen	
Comparison of Mechanical Properties of NiO/YSZ by Different Methods	361
Dustin R. Beeaff, S. Ramousse, and Peter V. Hendriksen	
Fracture Toughness and Slow Crack Growth Behavior of Ni-YSZ and YSZ as a Function of Porosity and Temperature	373
M. Radovic, E. Lara-Curzio, and G. Nelson	
Effect of Thermal Cycling and Thermal Aging on the Mechanical Properties of, and Residual Stresses in, Ni-YSZ/YSZ Bi-Layers	383
E. Lara-Curzio, M. Radovic, R. M. Trejo, C. Cofer, T. R. Watkins, and K. I. More	
Three-Dimensional Numerical Simulation Tools for Fracture Analysis in Planar Solid Oxide Fuel Cells (SOFCs)	393
Janine Johnson and Jianmin Qu	

Modeling

Electrochemistry and On-Cell Reforming Modeling for Solid Oxide Fuel Cell Stacks K. P. Recknagle, D. T. Jarboe, K. I. Johnson, V. Korolev, M. A. Khaleel, and P. Singh	409
Modeling of Heat/Mass Transport and Electrochemistry of a Solid Oxide Fuel Cell Yan Ji, J. N. Chung, and Kun Yuan	419
Author Index	435

Preface

The third international symposium “Solid Oxide Fuel Cells: Materials and Technology” was held during the 30th International Conference on Advanced Ceramics and Composites in Cocoa Beach, FL, January 22–27, 2006. This symposium provided an international forum for scientists, engineers, and technologists to discuss and exchange state-of-the-art ideas, information, and technology on various aspects of solid oxide fuel cells. A total of 125 papers, including three plenary lectures and eleven invited talks, were presented in the form of oral and poster presentations indicating strong interest in the scientifically and technologically important field of solid oxide fuel cells. Authors from four continents and 14 countries (Brazil, Canada, Denmark, France, Germany, India, Iran, Italy, Japan, Sweden, Switzerland, Taiwan, Ukraine, and U.S.A.) participated. The speakers represented universities, industries, and government research laboratories.

These proceedings contain contributions on various aspects of solid oxide fuel cells that were discussed at the symposium. Forty one papers describing the current status of solid oxide fuel cells technology and the latest developments in the areas of fabrication, characterization, testing, performance analysis, long term stability, anodes, cathodes, electrolytes, interconnects and protective coatings, sealing materials and design, interface reactions, mechanical properties, cell and stack design, protonic conductors, modeling, etc. are included in this volume. Each manuscript was peer-reviewed using the American Ceramic Society review process.

The editor wishes to extend his gratitude and appreciation to all the authors for their contributions and cooperation, to all the participants and session chairs for their time and efforts, and to all the reviewers for their useful comments and suggestions. Financial support from the American Ceramic Society is gratefully acknowledged. Thanks are due to the staff of the meetings and publications departments of the American Ceramic Society for their invaluable assistance. Advice, help and cooperation of the members of the symposium’s international organizing committee (Tatsumi Ishihara, Tatsuya Kawada, Nguyen Minh, Mogens Mogensen,

Nigel Sammes, Prabhakar Singh, Robert Steinberger-Wilkens, and Jeffrey Stevenson) at various stages were instrumental in making this symposium a great success.

It is our earnest hope that this volume will serve as a valuable reference for the engineers, scientists, researchers and others interested in the materials, science and technology of solid oxide fuel cells.

NAROTTAM P. BANSAL

Introduction

This book is one of seven issues that comprise Volume 27 of the Ceramic Engineering & Science Proceedings (CESP). This volume contains manuscripts that were presented at the 30th International Conference on Advanced Ceramic and Composites (ICACC) held in Cocoa Beach, Florida January 22–27, 2006. This meeting, which has become the premier international forum for the dissemination of information pertaining to the processing, properties and behavior of structural and multi-functional ceramics and composites, emerging ceramic technologies and applications of engineering ceramics, was organized by the Engineering Ceramics Division (ECD) of The American Ceramic Society (ACerS) in collaboration with ACerS Nuclear and Environmental Technology Division (NETD).

The 30th ICACC attracted more than 900 scientists and engineers from 27 countries and was organized into the following seven symposia:

- Mechanical Properties and Performance of Engineering Ceramics and Composites
- Advanced Ceramic Coatings for Structural, Environmental and Functional Applications
- 3rd International Symposium for Solid Oxide Fuel Cells
- Ceramics in Nuclear and Alternative Energy Applications
- Bioceramics and Biocomposites
- Topics in Ceramic Armor
- Synthesis and Processing of Nanostructured Materials

The organization of the Cocoa Beach meeting and the publication of these proceedings were possible thanks to the tireless dedication of many ECD and NETD volunteers and the professional staff of The American Ceramic Society.

ANDREW A. WERESZCZAK
EDGAR LARA-CURZIO
General Editors

Oak Ridge, TN (July 2006)

Overview and Current Status

DEVELOPMENT OF TWO TYPES OF TUBULAR SOFCs AT TOTO

Akira Kawakami, Satoshi Matsuoka, Naoki Watanabe, Takeshi Saito, Akira Ueno
TOTO Ltd.
Chigasaki, Kanagawa 253-8577 Japan

Tatsumi Ishihara
Kyushu University
Higashi, Nishi 819-0395 Japan

Natsuko Sakai, Harumi Yokokawa
National Institute of Advanced Industrial Science and Technology (AIST)
Tsukuba, Ibaraki 305-8565 Japan

ABSTRACT

The current status of two types of SOFC R & D at TOTO is summarized. We have developed 10kW class tubular SOFC modules for stationary power generation using Japanese town gas (13A) as fuel. A small module which consisted of 5 stacks (a stack consisted of 2 x 6 cells) generated 1.5kW at 0.2A/cm² and achieved 55%-LHV efficiency at an average temperature of 900°C. A thermally self-sustaining module consisting of 20 stacks achieved 6.5kW at 0.2A/cm² and 50%-LHV.

We have also developed micro tubular SOFCs for portable application, which operate at relatively lower temperatures. The single cell generated 0.85, 0.70, and 0.24W/cm² at 700°C, 600°C, and 500°C, respectively. We built and evaluated a stack consisting of 14 micro tubular cells, and it successfully demonstrated 43W, 37W and 28W at a temperature of 700°C, 600°C, and 500°C, respectively.

INTRODUCTION

TOTO is the top sanitary ware manufacturer in Japan and highly experienced in traditional and advanced ceramic products. Solid Oxide Fuel Cells (SOFCs) are mainly composed of ceramics, and our fabrication technology has been utilized to produce high performance SOFCs at a low cost. TOTO started the research and development of tubular type SOFCs in 1989. From 2001 to 2004, we successfully completed a 10kW class thermally self-sustaining module test in a New Energy and Industrial Technology Development Organization (NEDO) project. Since 2004, TOTO started a new collaboration with Kyushu Electric Power Co., Inc. and Hitachi, Ltd. in a new NEDO project. We are developing a co-generation system by integration with the TOTO stack. On the other hand, TOTO also started the development of micro SOFCs using micro tubular cells (diameter is less than 5mm) from 2002 under another NEDO project. In this paper, we summarized the current status of two types of SOFCs R & D at TOTO, i.e. tubular SOFC for stationary power generation and micro tubular SOFC for portable power application.

TOTO TUBULAR SOFC

Cell development

The schematic viewgraphs of the TOTO tubular cell are shown in Figure 1. A perovskite cathode tube is formed by extrusion molding. A zirconia electrolyte and a nickel/zirconia cermet

Development of Two Types of Tubular SOFCs at TOTO

anode are coated onto the tube by the TOTO uet process”. A vertical interconnector is coated along the tube in a strip. The diameter of the cell is 16.5mm and the active length is 660mm. Fuel gas is supplied to the outside of the cell, and air is supplied to the inside by a thinner air supply tube. Recently, the materials used for cells are changed as shown in Table 1. The neu material configuration resulted in the improvement of cell performance as shown in Figure 2, especially in lower operating temperatures. Our latest cell worked best at temperatures over 850°C.

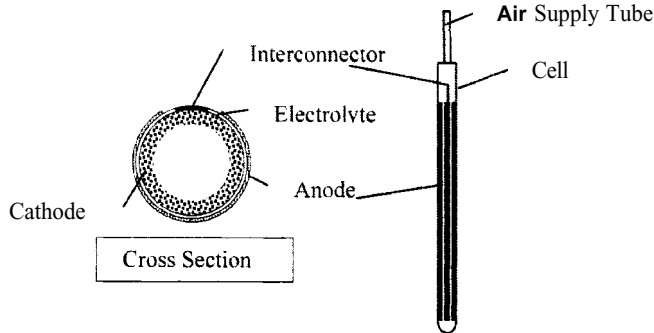


Figure 1. Schematic view of TOTO tubular cell.

Components	Previous Type Cell	New Type Cell
Cathode Tube	(La,Sr)MnO ₃	(La,Sr)MnO ₃
Electrolyte	YSZ	SCSZ
Anode	Ni/YSZ	Ni/YSZ
Interconnector	(La,Ca)CrO ₃	(La,Ca)CrO ₃

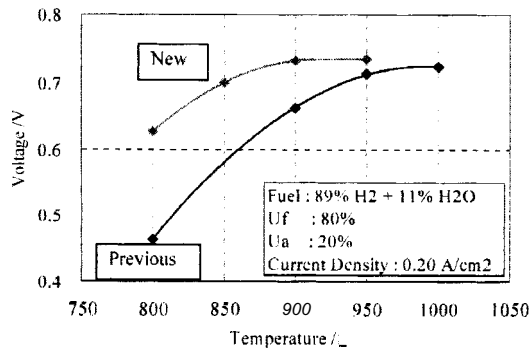


Figure 2. Cell performances as a function of operating temperature.

Stack development

Twelve tubes are bundled in a 2x6 stack with nickel materials connecting an interconnector of one cell and the anode of the next (Figure 3). A stack was installed in a metal casing and heated by an electric furnace. Simulated fuel of partially steam reformed town gas was supplied to the stack. The town gas was assumed to be 50% steam reformed under *SIC* (steam carbon ratio) =3.0. A stack generated 0.34kW at a current density of 0.2A/cm² at a temperature of 940°C. The maximum efficiency for DC output of the stack was 57%-Lower Heating Value (LHV) calculated on the basis of equivalent town gas (Figure 4).

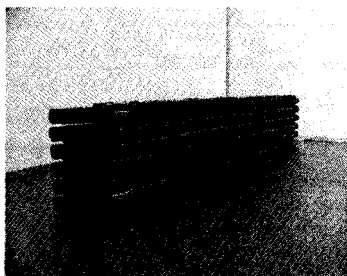


Figure 3. Appearance of TOTO stack.

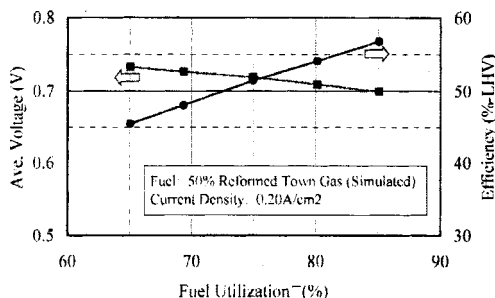


Figure 4 Performance of 2x6 stack.

Small module (quarter size module)

The thermally self-sustaining operation indicates that the modules generate power without any external heat supply. A quarter-size small size modules, which consisted of 5 stacks were made and tested for basic evaluations to realize the thermally self-sustaining operation. The small module and its metal casing were covered with a ceramic insulator. In this test, the desulfurized town gas was partially steam reformed through a reactor. The reformer was installed outside of the module with an electric furnace as shown in Figure 5. The conversion of steam

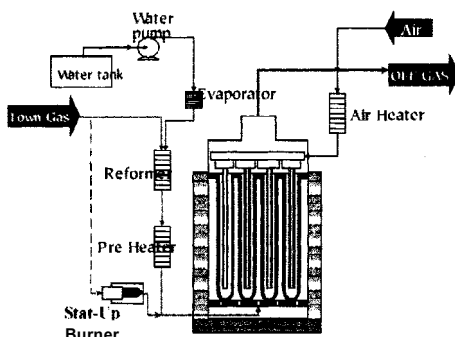


Figure 5. Flow diagram of small SOFC module.

reforming can be controlled independently with reformer temperature. However the higher hydrocarbons such as ethane (C_2H_6), propane (C_3H_8) and butane (C_4H_{10}) were completely converted. The residual CH_4 was internally reformed on the anode, and the endothermic effect was utilized to maintain the homogeneous temperature distribution of the module. The outlet fuel and air were mixed and burned above the module, and this combustion heat was used for air pre-heating. Those improvements in temperature distribution and fuel gas distribution strongly affected on the module performance. We succeeded to operate a module with 1.6kW at $0.2A/cm^2$ at an average temperature of $900^\circ C$ which corresponds to the efficiency of 40%-LHV for 3000 hours. The maximum efficiency was 55 %-LHV, which obtained for different module.

Thermally self-sustaining module

A ten kW class module consisting of four quarter-size modules is fabricated for thermally self-sustaining operation (Figure 6). An integrated heat exchanging steam reformer was mounted above the module. It consisted of an evaporator, pre-heater and reformer. However, the stability of the evaporator was not clearly demonstrated, therefore steam was supplied by another evaporator with an electric furnace. The gas flow was simple, and it does not include any gas recycles as shown in Figure 7. The module, the after-burning zone, and the reformer were covered with a ceramic insulator. A commercial steam reforming catalyst was embedded in the reforming section. The desulfurized town gas was supplied to the modules after being partially steam reformed. In the test, the heat of exhaust gases was used for steam reforming through the reformer. The module was heated by a partially oxidation burner and air heaters from room temperature.

The voltages of each stack, and of the 2-cells in a quarter module, were monitored, and the variation of the voltages was quite small. The module generated 6.5kW at $0.19A/cm^2$ and 46%-LHV (Table 2 Test 1). The improved module generated 6.5kW at $0.2A/cm^2$ and 50%-LHV (Table 2 Test 2). The thermally self-sustainability of both operating condition were confirmed. The test was shifted to evaluation of long-term stability under the condition of Test 1. No degradation was observed in the module or the integrated heat exchanging steam reformer during the operating time of 1000 hours (Figure 8).

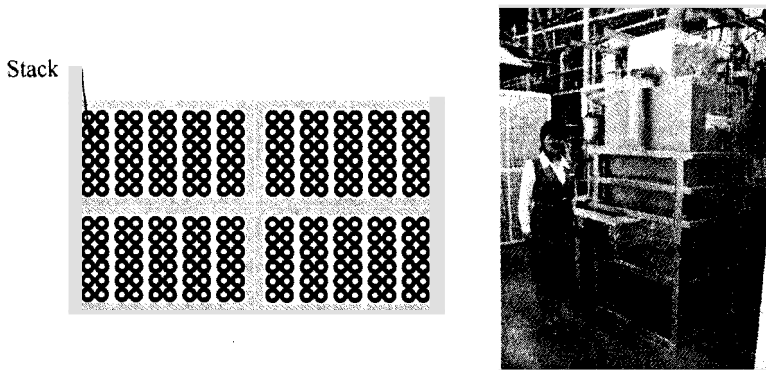


Figure 6. Stack layout and appearance of thermally self-sustaining SOFC module.

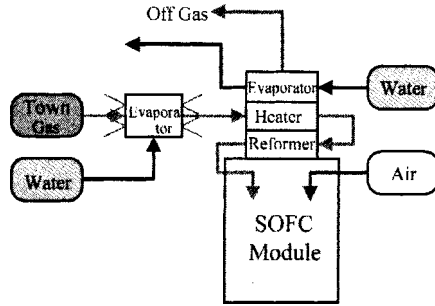


Figure 7. Flow diagram of thermally self-sustaining SOFC module system.

Table 2. Performance of thermally self-sustaining SOFC module.

Items	Test 1	Test 2
Power(kW)	6.4	6.5
Uf (Yo)	70	75
Current Density (A/ cm ²)	0.19	0.20
Ave. Cell Voltage (V)	0.69	0.70
Efficiency(%-LHV)	46	50

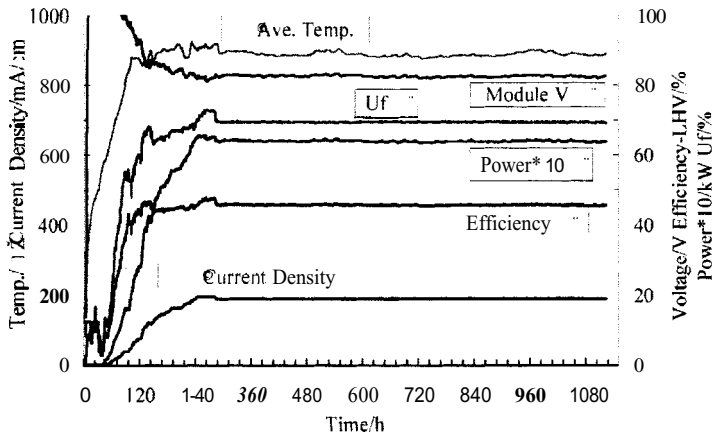


Figure 8. Long term stability of thermally self-sustaining SOFC module.

Development of Two Types of Tubular SOFCs at TOTO

Component	Material	Fabrication	Firing
Anode Tube	NiO/YSZ	Extrude Molding	Co-Firing
Anode Interlayer	NiO/GDC 10	Slurry coating	
Electrolyte	LDC40(Ga ₂ O ₃)-LSGM (Double Layered)		
Cathode	LSCF		Firing

Figure 9 is a picture of a micro tubular single cell. The diameter of cell is 5mm, and the active length is 50mm. The single cell was jointed to the current collector cap with silver braze metal and its performance was tested in a furnace. Figure 10 shows the evaluation method for single cell performance. A fuel gas was supplied inside the cell, and air was supplied to the outside of the cell. The current voltage and impedance of the single cells were measured using a potentiostat and a frequency response analyzer in the 500 to 700°C temperature range.

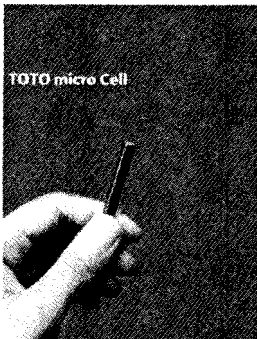


Figure 9. TOTO micro tubular cell.

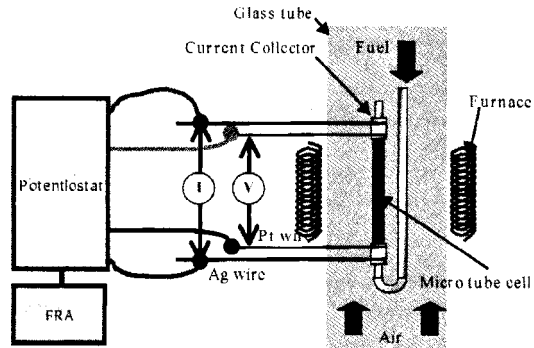


Figure 10. Evaluation method for single cell performance.

Figure 11 show the typical I-V curves of a micro tubular single cell using dry H_2 in N_2 as fuel. H_2 flow was fixed at 0.12L/min. The open circuit voltage (OCV) was close to the theoretical value. It indicated that the electrolyte has a good gas tightness, and the chemical reaction between LSGM and Ni are effectively avoided by the LDC40 layer. The maximum

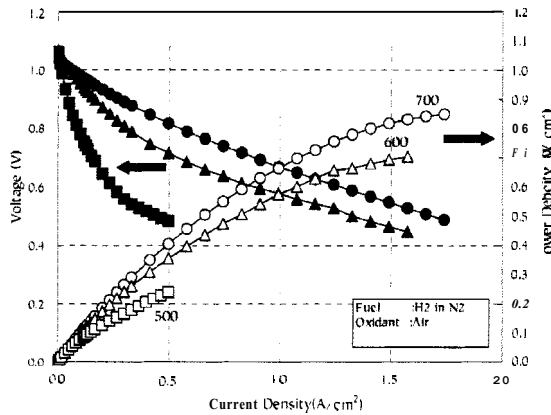


Figure 11. I-V characteristic of micro tubular single cell.

power densities were 0.85, 0.70, and 0.24 W/cm² at 700°C, 600°C, and 500°C, respectively. Figure 12 shows the impedance spectra of a micro tubular cell measured under 0.125 A/cm² at various temperatures. It has been generally assumed that the intercept with the real-axis at the highest frequency represents the ohmic resistance, and the width of low frequency arc represents the electrode resistance. The electrode resistance increased significantly with decreasing operation temperature, and ohmic resistance at 500°C was very high. The most likely cause of the high resistance is the low ionic conductivity of LDC40. Therefore, it is expected that the cell performance can be improved by optimizing the anode electrode and the thickness of LDC40 layer.

Figure 13 shows the fuel utilization effects on micro tubular cell performance measured under 0.125 A/cm² at 700°C and 600°C. The observed cell voltage was close to the theoretical value calculated by the Nernst equation. It indicates that the micro tubular cell can be operated at a high efficiency.

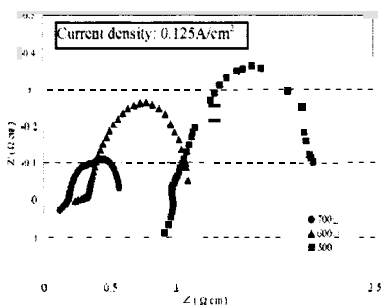


Figure 12. Impedance of micro tubular cell.

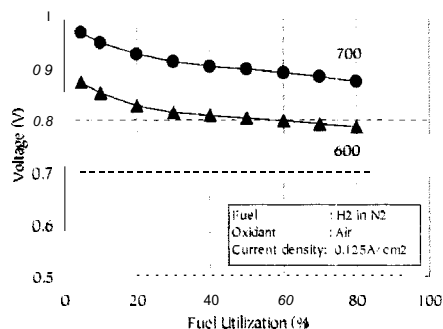


Figure 13. Fuel utilization effect on micro tubular cell performance.

The cell performances using H₂ in N₂ (1:1) gas mixture or simulated reformate gas were compared in Figure 14. The composition of simulated reformate was 32% H₂, 13% CO, 5% CO₂, and 50% N₂ based on the preliminary experiment of the catalytic partial oxidation (CPOX) reforming of LPG. As shown in the figure, the difference in cell performances was small at lower current densities. However, the performance using reformate gas was lower at higher current densities at temperatures of 600°C and 700°C. The differences became significant with increasing operating temperatures. To identify the differences, the impedance spectra were measured under a current density of 0.8 A/cm² at 700°C (Figure 15). The electrode resistance on simulated reformate was higher than that on H₂ in N₂, and it was thought that this difference was caused by the CO transport resistance from the anode in the high current density area. Therefore, we are now trying to improve the anode performance.

Figure 16 shows the cell performance using DME + air mixture as fuel at 550°C. The DME flow rate was fixed at 85 ml/min and the excess air ratios (air-fuel ratio/theoretical air-fuel ratio) were 0.1, 0.2, 0.3, and 0.4 respectively. Direct use of fuel without a reformer in SOFCs will simplify the system greatly, and this is important for SOFCs, especially in portable and transportation applications. DME is an attractive fuel because it is highly active and easily

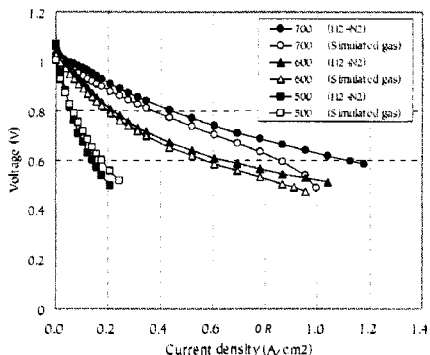


Figure 14. I-V curve tested on H₂ in N₂ and simulated reformat gas.

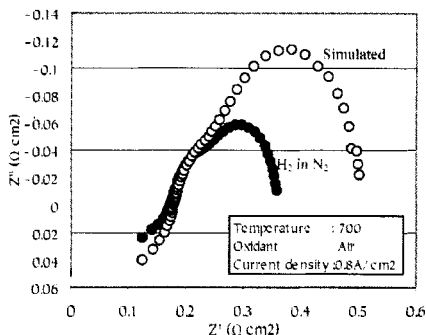


Figure 15. Impedance tested on H₂ in N₂ and simulated reformat gas.

liquefied and stored. As shown in the figure, the use of DME + air as fuel resulted in higher performance than that of H₂ in N₂ and no carbon deposition was observed during operation. Figure 17 shows the DME conversion rate and the exhaust gas composition analyzed by a gas chromatography. (The water content was not measured.) The DME conversion rate and CO₂ content increased with excess air ratio. Therefore, the increased performance achieved by using DME + air mixture is probably due to the raising cell surface temperatures caused by the decomposition and the combustion of DME. (The furnace temperature was kept at 550°C). These results demonstrated the high possibility of micro tubular cells being used for direct fueled operations

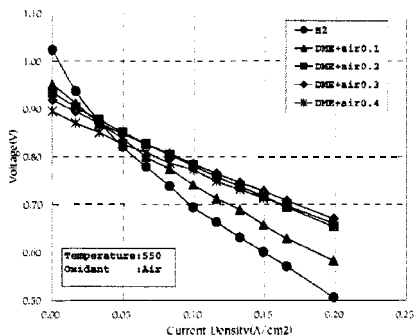


Figure 16. I-V curve tested on DME+air mixture as fuel at 550°C.

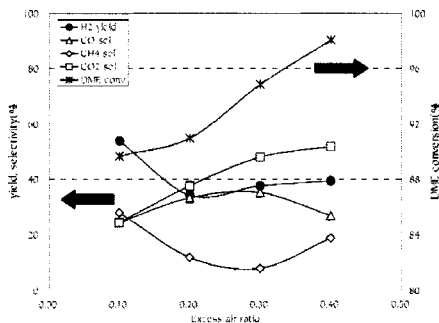


Figure 17. DME conversion rate and exhaust gas composition tested on DME+air mixture.

Micro tubular stack development

In order to evaluate the performance of cells in a bundle, we built the stack consisting of 14 micro tubular cells as shown in Figure 18. This stack was evaluated in a furnace using hydrogen as a fuel, and successfully demonstrated 43 W, 37 W and 28 W power generation at a temperature of 700°C, 600°C, and 500°C, respectively (Figure 19). Table 4 summarizes the results we have obtained from the stack evaluation. The maximum stack power densities were 478 W/L and 239 W/kg at 700°C. These results demonstrated that micro tubular SOFCs have a high potential for portable and transportation applications.

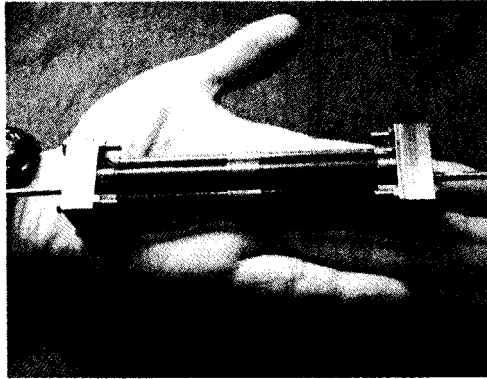


Figure 18. Appearance of micro tubular SOFC stack.

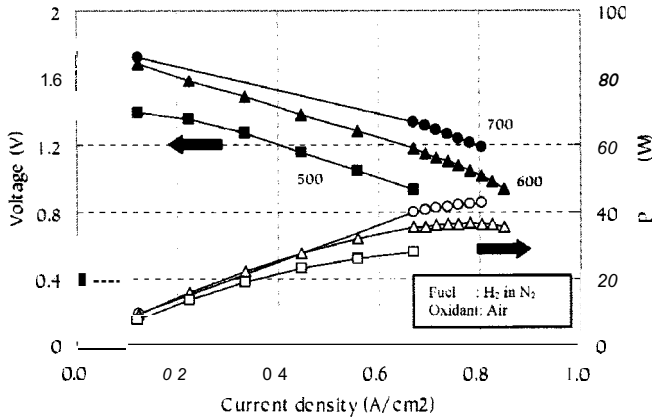


Figure 19. Performance of micro tubular SOFC stack.

Table 4. Performance of micro tubular SOFC stack at 700°C.

Item	Result
Maximum power (W)	43
Stack volume (L)	0.09
Stack weight (kg)	0.18
Stack power density (W/L)	478
Stack power density (W/kg)	239

SUMMARY

TOTO tubular SOFC

The 2x6 stack, small module and thermally self-sustaining module of the TOTO tubular SOFC were designed and made. They were evaluated using town gas or simulated fuel and showed excellent performance. We continually improve the cell performance and the durability to advance the module performance. TOTO started the small-scale production of SOFC and trial delivery in 2004. The SOFC can be supplied as a stack for the development of stationary power generation systems. In 2004, TOTO started a new collaboration with Kyushu Electric Power Co., Inc. and Hitachi, Ltd. in a new NEDO project. We are developing a co-generation system by integration with the TOTO stack.

TOTO micro tubular SOFC

The anode-supported micro tubular cells with thin lanthanum gallate with strontium and magnesium doping were developed. The single cells and the cell stack were tested using various fuels, i.e. hydrogen, simulated reformat gas of LPG, direct fueling of DME, and they showed excellent performance at lower temperatures from 500-700°C. These results demonstrated that micro tubular SOFCs have a high potential for portable and transportation applications. Further development on durability, quick start up, and compactness of the stack is being undertaken.

ACKNOWLEDGMENT

The development was supported by NEDO in Japan.

REFERENCES

- ¹T. Saito, T. Abe, K.Fujinaga, M. Miyao, M. Kuroishi, K. Hiwatashi, A. Ueno, "Development of Tubular SOFC at TOTO", SOFC-IX, Electrochemical Society Proceedings Volume 2005-07, 133-140(2005)
- ²K. Hiwatashi, S.Furuya, T. Nakamura, H. Murakami, M. Shiono, M. Kuroishi, "Development Status of Tubular type SOFC by Wet Process", Proc. of the 12th Symposium on Solid Oxide Fuel Cells in Japan, 12-15(2003)
- ³J. Van herle, J. Sfeir, R. Ihringer, N. M. Sammes, G. Tompsett, K. Kendall, K. Yamada, C. Wen, M. Ihara, T. Kawada and J. Mizusaki, "Improved Tubular SOFC for Quick Thermal Cycling", Proc. of the Fourth European Solid Oxide Fuel Cell Forum, 251-260 (2000)
- ⁴A. Kawakami, S. Matsuoka, N. Watanabe, A. Ueno, T. Ishihara, N. Sakai, K. Yamaji, H. Yokokawa, "Development of low-temperature micro tubular type SOFC", Proc. of the 13th Symposium on Solid Oxide Fuel Cells in Japan, 54-57(2004)
- ⁵T. Ishihara, H. Matsuda, Y. Takita, "Doped LaGaO₃ perovskite type oxide as a new oxide ionic conductor", J. Am. Chem. Soc, 116, 3801-3803 (1994)
- ⁶M.Feng, J.B.Goodenough, "A superior oxide-ion electrolyte", Eur. J. Solid State Inorg. Chem., 31, 663-672 (1994)
- ⁷K. Huang, J.H Wan, J.B.Goodenough, "Increasing Power Density of LSGM-Based Solid Oxide Fuel Cells Using New Anode Materials", J. Electrochem. Soc, 148(7), A788-A794 (2001)

Cell and Stack Development

DEVELOPMENT OF SOLID OXIDE FUEL CELL STACK USING LANTHANUM GALLATE-BASED OXIDE AS AN ELECTROLYTE

T. Yamada, N. Chitose, H. Etou, M. Yamada, K. Hosoi and N. Komada
Mitsubishi Materials Corporation, Fuel Cell Group, Business Incubation Department
1002-14 Mukohyama, Naka, Ibaraki, 311-0102, Japan

T. Inagaki, F. Nishiwaki, K. Hashino, H. Yoshida, M. Kawano and S. Yamasaki
The Kansai Electric Power Company, Inc., Energy Use R&D Center
11-22 Nakoji, 3-chome, Amagasaki, Hyogo, 661-0974, Japan

T. Ishihara
Department of Applied Chemistry, Faculty of Engineering, Kyushu University
744 Motoooka, Nishi-ku, Fukuoka, 819-0395, Japan

ABSTRACT

One of the important trends in recent years is to reduce the operating temperature of solid oxide fuel cell (SOFC). Since FY2001, Mitsubishi Materials Corporation (MMC) and The Kansai Electric Power Co., Inc. (KEPCO) have been collaborating to develop intermediate temperature SOFC modules, which use lanthanum gallate based electrolyte, for stationary power generation.

Our recent study has been focused on the durability of the stack repeat unit which is composed of a disk-type electrolyte-supported cell, an anode-side current collector, a cathode-side current collector and two interconnects, and on the improvement of the output power density of the cell. A long-term test of a stack repeat unit has been performed at 750 °C under constant current density of 0.3 A/cm² with hydrogen flow rate of 3 ml/min/cm² and air flow rate of 15 ml/min/cm² for over 10,000 hrs. The decrease in terminal voltage was not observed the initial 2,000 hrs, but was 1–2 %/1,000 hrs after then. The maximum electrical efficiency attained was 54 % (LHV) at 750 °C and 0.292 W/cm² with 90 % hydrogen utilization.

The third-generation 1-kW class module was operated as CHP demonstration system for 2,000 hrs without significant degradation.

The fourth-generation 1-kW class module successfully provided the output power of 1 kW with thermally self-sustained operation below 800 °C. The average electrical efficiency calculated from the experimental data for 21 hrs stable operation was 60 % (LHV).

INTRODUCTION

A solid oxide fuel cell (SOFC) is an energy conversion device receiving great deal of interest because of its high electrical efficiency, environmental compatibility, and ability to utilize variety of fuels. However, there are a number of problems before realizing a low-cost high-performance SOFC, arising from the high operating temperature as high as 1,000 °C. A reduction in operating temperature (<800 °C) in SOFC can decrease materials degradation and facilitate the use of low-cost metallic components for interconnect? etc. instead of more expensive ceramic materials.

Recently Ishihara et al. reported a reduced-temperature SOFC using the perovskite-type oxide of doped LaGaO₃ as electrolyte^[1]. In particular, LaGaO₃ where Sr was substituted for the

Development of Solid Oxide Fuel Cell Stack Using Lanthanum Gallate-Based Oxide

La-site and Mg and Co for the Cia-site ($\text{La}_{0.8}\text{Sr}_{0.2}\text{Ga}_{0.8}\text{Mg}_{0.2-x}\text{Co}_x\text{O}_{3-\delta}$)^[2,3] was highly interesting from the viewpoint of decreasing the operating temperature.

Mitsubishi Materials Corporation (MMC) and The Kansai Electric Power Co., Inc. (KEPCO) have been collaborating to develop intermediate-temperature SOFC (IT-SOFC) modules, which use the above-mentioned lanthanum gallate-based electrolyte, for stationary power generation units since FY2001. The target of the development for the forthcoming several years is to commercialize 10-kW class high-efficiency IT-SOFC module. The module of this particular size is being designed and constructed by MMC and will be integrated into the combined heat and power (CHP) generating system which is subsequently being developed by KEPCO under New Energy and Industrial Technology Development Organization (NEDO) program.

In this paper, the performances of the SOFC stack repeat unit and the recent generations of 1-kW class modules operated at intermediate temperatures are reported.

EXPERIMENTAL

The electrolyte powder mixture is prepared by using the conventional solid state reaction technique with commercially available starting powders of La_2O_3 (99.99 %), SrCO_3 (99.9 %), Ga_2O_3 (99.99 %), MgO (99.99 %) and CoO (99 %). In particular, these commercial powders were mixed proportionally to the composition of $\text{La}_{0.8}\text{Sr}_{0.2}\text{Ga}_{0.8}\text{Mg}_{0.15}\text{Co}_{0.05}\text{O}_{3-\delta}$ (LSGMC) by ball-milling and then calcined at 1,200 °C in air. The calcined powders were ground again and mixed with a binder and an organic solvent for 1 day, and the prepared slurry was tape-cast to make green sheet. After drying, disks were cut out from the sheets, and sintered at 1,400–1,500 °C in air after removing organic additives at temperatures lower than 1,000 °C. The thickness of the sintered specimens were 200–250 μm, and their densities were larger than 98 % of the theoretical value.

$\text{Ni/Ce}_{0.8}\text{Sm}_{0.2}\text{O}_{2-\delta}$ (Ni/SDC) and $\text{Sm}_{0.5}\text{Sr}_{0.5}\text{CoO}_{3-\delta}$ (SSC) were used for the anode and the cathode, respectively. The area of 113.1 cm² (φ120 mm) was first coated with a slurry of a mixture of the anode powders and an organic binder on a surface of the electrolyte, followed by calcination at 1,200–1,300 °C in air. Then, the cathode was coated similarly on the opposite surface of the electrolyte, followed by calcination at 1,100–1,200 °C. Disk-type electrolyte-supported cells are shown in Figure 1.

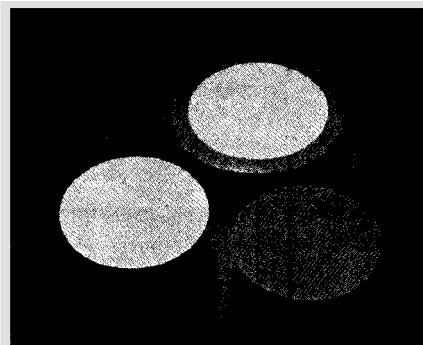


Figure 1 Disk-type electrolyte-supported cells

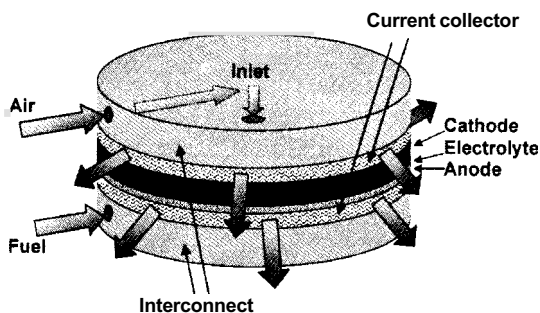


Figure 2. Schematic illustration for the disc-type seal-less SOFC stack repeat unit.

For the power-generation experiment, the seal-less stack repeat unit shown in Figure 2 was used. As current collectors, porous metallic sheets were attached to the electrodes. The current collectors were sandwiched between separators made of ferritic stainless steel with special surface treatment to maintain contact resistances within acceptable levels and the cell. The electric current was taken out directly from the interconnects. The stack repeat unit set with a test cell was placed in a uniform temperature field generated by electric heater plates. Dry hydrogen was preheated and supplied to the anode regulated by a mass flow controller. Air was preheated and supplied to the cathode regulated by a floater-type flow meter at a volumetric rate at five times of hydrogen flow. All power generation tests were carried out at 650, 700, 750 and 800 °C with typical voltage-current measurements starting from the open circuit voltage (OCV) down to 0.5 V.

PERFORMANCES OF THE STACK REPEAT UNITS

Figure 3 shows the temperature dependence of the electrical conductivities of doped lanthanum gallate and stabilized ZrO₂. It is noted that the electrical conductivity of La_{0.8} Sr_{0.2} Ga_{0.8} Mg_{0.1} Co_{0.1} O_{3-δ} is much higher than that of the conventional electrolytes.

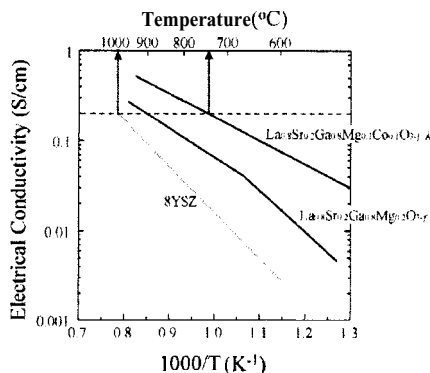


Figure 3. Electrical conductivity of various oxides.

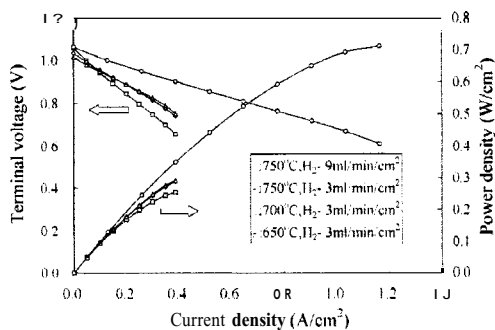


Figure 4. Voltage-current characteristics of the stack repeat unit.

For a given thickness, the same level of electrical conductivity with other materials can be achieved at much lower temperatures when $\text{La}_{0.8}\text{Sr}_{0.2}\text{Ga}_{0.8}\text{Mg}_{0.1}\text{Co}_{0.1}\text{O}_{3-\delta}$ is used as an electrolyte.

Figure 4 shows the typical power generating characteristics of the stack repeat unit at 650–750 °C. It is observed that the output power density was 0.248 W/cm^2 at 0.3 A/cm^2 and 750°C with 70 % hydrogen utilization under air flow rate of 15 ml/min/cm^2 and dry hydrogen flow rate of 3 ml/min/cm^2 . And thus, the electrical efficiency was 45.8 % (LHV). The maximum output power density of 0.71 W/cm^2 was attained at 1.2 A/cm^2 and 750 °C with 90 % hydrogen utilization under air flow rate of 45 ml/min/cm^2 and dry hydrogen flow rate of 9 ml/min/cm^2 . The corresponding electrical efficiency was 43 % (LHV). Table 1 summarizes the typical power generating characteristics of the stack repeat unit as a function of temperature. The data correspond to measurements performed at a specified current density and fuel utilization (U_f) for temperatures between 650 °C and 800 °C (see columns 2,3,4,5). On the other hand, the column number 6 is for values obtained for the highest conversion efficiency and the column number 7 is for the maximum power density at 750 °C. Although the peak output power was achieved at 750°C, the variation in terminal voltage at 0.3 A/cm^2 and U_f 70 % was only a few percent in the temperature range between 700 and 800 °C. Therefore, it is confirmed from these experiments that the operating temperature of the SOFC may be decreased to ca. 700 °C without compromising the performance of cells developed in the current program.

Table 1. Typical performances of the stack repeat unit.

Temperature (°C)	650	700	750	800	750	750
H ₂ flow rate (ml/min/cm ²)	3	3	3	3	3	9
Fuel utilization (%)	70	70	70	70	90	84
Terminal voltage (V)	0.748	0.815	0.825	0.816	0.751	0.668
Output power (W)*	25.4	27.7	28.0	27.7	33.0	78.2
Current density (A/cm ²)	0.30	0.30	0.30	0.30	0.39	1.04
Power density (W/cm ²)	0.225	0.245	0.248	0.245	0.292	0.692
Efficiency (%LHV)	41.5	45.2	45.8	45.3	53.9	42.7

Despite the fact that the cells are capable of generating much higher power densities, we decided to operate them at lower power densities and lower fuel utilizations for eliminating complexities such as cell degradation, heat management etc.

A long-term test of a stack repeat unit has been done at 750 °C and 0.3 A/cm² with hydrogen flow rate of 3 ml/min/cm² and air flow rate of 15 ml/min/cm² for over 10,000 hrs. The variation in terminal voltage is shown in Figure 5. It was found that no decrease in terminal voltage occurred during the initial 2,000 hrs. However, during the rest of the test period the decrease in terminal voltage was 1~2 %/1,000 hrs.

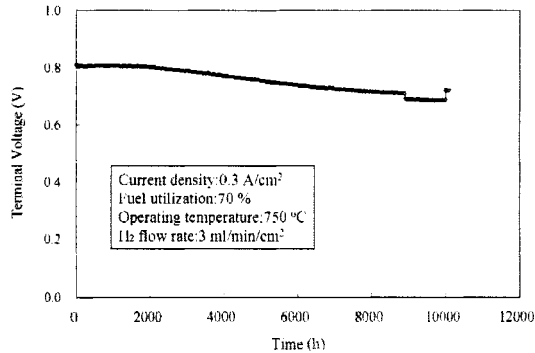


Figure 5. Variation of the terminal voltage during the stability test of the stack repeat unit.

PERFORMANCES OF THE 1-kW CLASS MODULE

Following the success of earlier 1-kW class modules, the third-generation 1-kW class module has been manufactured for CHP generation system demonstration. The module shown in Figure 6 contains a single-stack of 46 cells, a pre-reformer, a steam generator, and heat exchangers for fuel and air. Desulfurized town gas, deionized water, and air are supplied to the module at room temperature. Electric heaters are used for the initial start-up then turned off once the stack reached the temperature high enough for the steam-reforming and for the electrochemical reactions. During the thermally self-sustained operation, the stack temperature is controlled by adjusting the air flow rate.

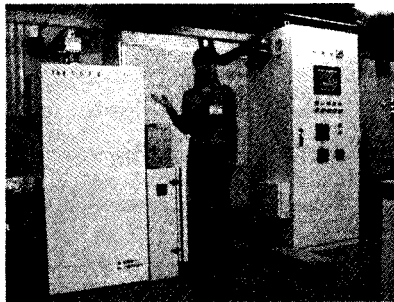


Figure 6. Demonstration system with the third-generation 1-kW class module.

Development of Solid Oxide Fuel Cell Stack Using Lanthanum Gallate-Based Oxide

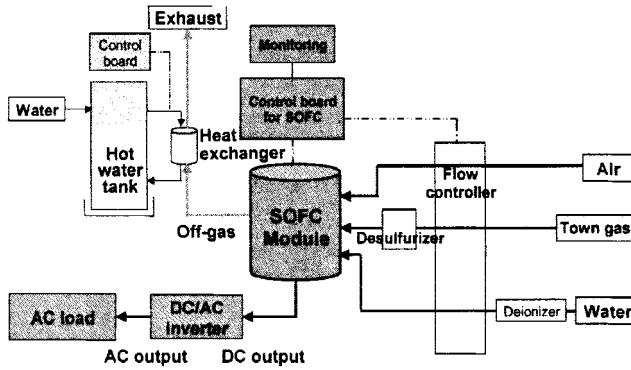


Figure 7. Schematic diagram of the 1-kW class demonstration system.

DC power output	1095W
AC power output	992W
Inverter efficiency	92%
DC conversion efficiency	56%(LHV)
AC conversion efficiency	51%(LHV)*2
S/C	3.5

of 90 °C was produced utilizing the module exhaust gas during the operation at AC output power of 1 kW.

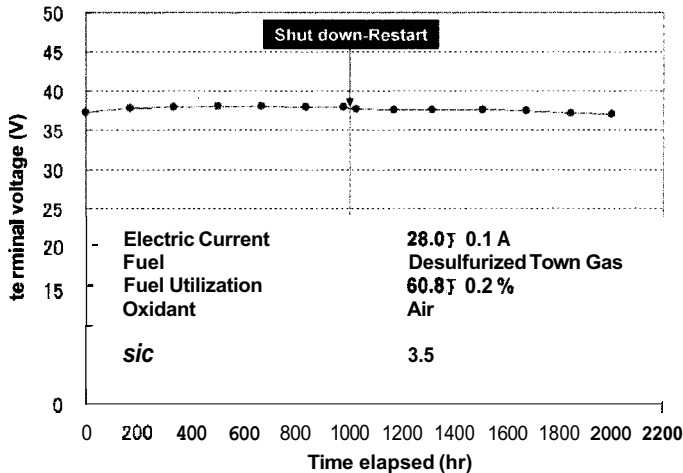


Figure 8. Long-term stability of the third-generation 1-kW class module.

A long-term stability test of the demonstration system was also performed. During the test, the system was controlled to provide 1 kW-AC power output. then the DC terminal voltage of the module was periodically measured at prescribed current and fuel flow rate. As shown in Figure 8, durability of the module over 2,000 hrs was demonstrated successfully.

The fourth and the latest generation module confirmed the integrity of the design concept of the cell stack and the hot BoP components such as pre-reformer, steam generator, and heat exchanger of both air and fuel built within the module. The external view of the module is shown in Figure 9.

One of the major design improvements from the earlier generations to the fourth generation was the optimization of both temperature profile and heat-flux distribution within the module to attain higher efficiency. In order to complete this task for higher efficiency, in the fourth generation stack, a novel interconnect plate with internal gas manifolds was designed. The new design requires reduced number of stack components. Air and fuel inlets are situated at the opposite corners of the square interconnect plate. The interconnect plate is designed in such a way that the gas manifolds are constructed by stacking the interconnect plates and the ceramic rings alternately as shown in Figure 10. Stud bolts are used to fixate the entire stack between the end plates while providing the necessary compression for preventing gas leakage between ceramic rings and interconnects. Axial compressions needed for the gas manifolds and for the electrochemically active region are separated by introducing cantilevered arms to interconnect plates. With this elegant design, the axial compression applied to the electrochemically active region is optimized to minimize the contact resistances and at the same time to eliminate the possibility of mechanical failure of the stack components.

The DC power output of 1.160 W was recorded at the output terminals under thermally self-sustained and stable operation of the forth-generation module against the design target of 1.120 W. Desulfurized town gas was supplied to the module as fuel and air was utilized as oxidant at room temperature.

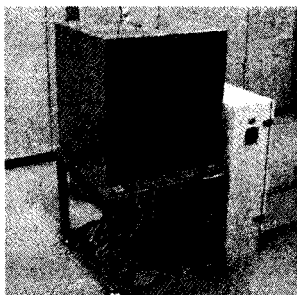


Figure 9. External view of the fourth-generation 1-kW class module.

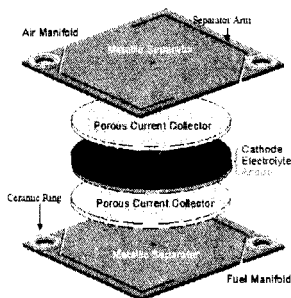


Figure 10. The fourth-generation stack unit design with internal gas manifolds

Deionized water was pumped into the module again at room temperature for steam reforming of the town gas, which was carried out within the module. The observed stack average temperature was 758 °C. The average conversion efficiency carefully calculated from the experimental data for the 21 hrs stable operation was 60%(LHV). The typical performance of the fourth generation module is shown in Table 3.

Fuel	Town gas*1
DC power output	1145W
DC current	31.9A
DC terminal voltage	35.9V
DC conversion efficiency	60%LHV
Fuel utilization	81%
Average stack temperature	758 °C
S/C	3.4

*1 CH₄:89%, C₂H₆:7%, C₃H₈:3%, C₄H₁₀:1%

CONCLUSIONS

We have characterized the power-generation of the stack repeat unit using LSGMC electrolyte in the temperature range between 650 and 800 °C. The maximum output power density of 0.71 W/cm² is attained at 1.2 A/cm² and 750 °C with 90 % hydrogen utilization under air flow rate of 45 ml/min/cm² and hydrogen flow rate of 9 ml/min/cm². The voltage drop was 1–2 %/1,000 hrs for 2,000–10,000 hrs at 750 °C and 0.3 A/cm² with 70 % hydrogen utilization under hydrogen and air.

The third-generation 1-kW class module was operated as CHP demonstration system for 2,000 hrs without significant degradation. The fourth-generation 1-kW class module was successfully constructed using interconnect plates with internal manifolds. Output power of 1-kW and the electrical efficiency of 60 % (LHV) with thermally self-sustained and stable operation was achieved below 800 °C.

ACKNOWLEDGEMENTS

Part of this work has been supported by the New Energy and Industrial Technology Development Organization (NEDO) under the "Development of Solid Oxide Fuel Cell System Technology" P04004 project.

REFERENCES

- ¹T. Ishihara et al., *J. Am. Chem. Soc.*, **116**, 3801 (1994).
- ²T. Yamada et al., *Sol. State Ionics*, **113-115**, 253 (1998).
- ³T. Ishihara et al., *Chem. Eng. Sci.*, **54**, 1535 (1999).
- ⁴T. Ishihara et al., *Sol. State Ionics*, **113-115**, 585 (1998).
- ⁵K. Kuroda et al., *Sol. State Ionics*, **132**, 199 (2000).
- ⁶N. Chitose et al., Proceedings International Hydrogen Energy Congress and Exhibition IHEC 2005 Istanbul, Turkey, (2005).
- ⁷T. Kotani et al., Abstracts for 2005 Fuel Cell Seminar, California, USA, 81 (1998).

ANODE SUPPORTED LSCM-LSGM-LSM SOLID OXIDE FUEL CELL

Alidad Mohammadi¹, Nigel M. Sammes², Jakub Pusz¹, Alevtina L. Smimova¹

¹Department of Materials Science and Engineering; University of Connecticut; 97 Eagleville Road; Storrs, CT 06269, USA

²Department of Mechanical Engineering; University of Connecticut; 191 Auditorium Road; Storrs, CT 06269, USA

ABSTRACT:

This paper describes an intermediate temperature solid oxide fuel cell (ITSOFC), based on porous $\text{La}_{0.75}\text{Sr}_{0.25}\text{Cr}_{0.5}\text{Mn}_{0.5}\text{O}_3$ (LSCM) anode, $\text{La}_{0.8}\text{Sr}_{0.2}\text{Ga}_{0.8}\text{Mg}_{0.2}\text{O}_{2.8}$ (LSGM) electrolyte, and porous $\text{La}_{0.6}\text{Sr}_{0.4}\text{MnO}_3$ (LSM) cathode. Using different amounts of poreformers, binders and firing temperatures, the porosity of the anode was optimized while still retaining good mechanical integrity. The effect of cell operation condition under saturated hydrogen fuel on the SOFC open circuit voltage (OCV) was also investigated. It is shown that 20 mL/min flow rate of saturated hydrogen results in an initial OCV up to about 1.0V for a single cell. The cell was tested for more than 500 hours maintaining high values of OCV (0.9V). Increasing the hydrogen flow rate up to 200 mL/min, results in enhanced OCV values up to 0.99V.

1. INTRODUCTION:

In conventional SOFCs Ni-zirconia cermet (NiO-YSZ) is used as the anode material while the electrolyte is yttria stabilized zirconia (YSZ) and the cathode is a strontium doped lanthanum manganite (LSM) [1,2,3]. Such a cell operates in the temperature range of 850-1000°C. However, the intermediate temperature operation conditions (600-800°C) not only reduce the cost, but also improve performance and the SOFC stack long-term endurance. In order to optimize the SOFC performance in the intermediate temperature range, the corresponding alternative materials can be used [4,5], such as ceria or lanthanum oxides that are cost effective alternatives for YSZ. The Gd_2O_3 doped CeO_2 (GCO) has higher ionic conductivity than YSZ [6,7] and lower thermal expansion coefficient than Co-based perovskites [8], which make it attractive for intermediate temperature SOFC electrolyte applications. However, the reduction of Ce^{4+} to Ce^{3+} can cause some electronic conduction, which results in a power loss [9]. Another alternative for YSZ electrolyte is Mg doped lanthanum gallite (LSGM) that is known to possess lower resistivity and higher ionic conductivity compared to that of YSZ [10,11]. High catalytic activity for oxygen dissociation and good chemical stability over wide range of oxygen partial pressures are other advantages of LSGM [10,12,13]. LSM can be used as a proper cathode material for LSGM electrolyte since there is no interfacial reaction reported between these two materials applying firing temperatures up to 1470°C [14], however the fabrication process is important to achieve proper cathode microstructure [15].

The goal of this work was to optimize the anode and cell structure considering both microstructural changes during sintering process and cell performance under OCV conditions.

2. EXPERIMENTAL PROCEDURE:

2.1. Manufacturing of anode pellets

Different amounts of poreformer were used for making pellets for anode support. Mixing of 5-10wt% potato fiber as poreformer with LSCM powder resulted in 40-50% porosity of anode supported pellets. Organic binder composition [16] was used in some samples in addition to the pore-former. In this case the LSCM powder was mixed with 5wt% of poreformer and 5wt% of binder. The mixture dried overnight, was heated for couple of hours at $100\pm 7^{\circ}\text{C}$, and then kept overnight again before grinding. The anode supported pellets were uniaxially pressed under 3500psi load and fired at 1200°C for 2 hrs.

2.2. Electrolyte supported cells preparation

Pellets of electrolyte were made using LSGM powder under applied pressure of 3500psi. These pellets were fired for 2 hrs at 1400°C . Anode slurry was made adding methanol to the mixture of LSCM powder and 5% potato fiber poreformer. This slurry was brushed on a surface of sintered electrolyte pellet and after drying at room temperature fired for 2 hrs at 1200°C . Then LSM cathode ink was painted on the other side of the pellet and after drying at room temperature fired at 1200°C for 2hrs. Compared to the anode supported cells, the electrolyte supported cells have the advantage of having higher porosity in anode layer since the electrolyte is fired first. Thus, lower anode sintering temperature results in higher mass transfer rate in anode.

2.3. Fuel cell testing procedure

The spiral silver wires used as current collectors were attached to the anode and cathode of the cell using Alfa Aesar silver conductive adhesive paste. The paste was cured at 150°C for 0.5-1 hour to obtain strong bonding and good contacts and then (Figure 1) the cell was attached to an alumina tube using sealant to prevent reaction between air and fuel mixtures. Ceramabond 552 from Aremco products, Inc. was used as the sealant. The sealant was dried at room temperature for 2 hrs and then cured for 2 hrs at 93°C and 2 hrs at 260°C . Steel tubes were sealed on the other end of the alumina tube to let the fuel in and out. Saturated hydrogen passing inside the tube was blown to the anode side, while air was blown to the cathode side using a small blower. The hydrogen flow rate was controlled using FCTS GMET gas box by Lynntech Industries. Ltd. and then hydrogen was passed through a humidifier at room temperature. The entire system, including a stainless steel tube to blow air to the cathode, was fitted in the furnace. The furnace was fired up to 800°C and kept at that temperature during the entire experiment. Both air and saturated hydrogen were blown initially while heating up the furnace and during the entire experiment. This experiment is repeated several times and the final results are the average of individual experiment's results.

Anode Supported LSCM-LSGM-LSM Solid Oxide Fuel Cell

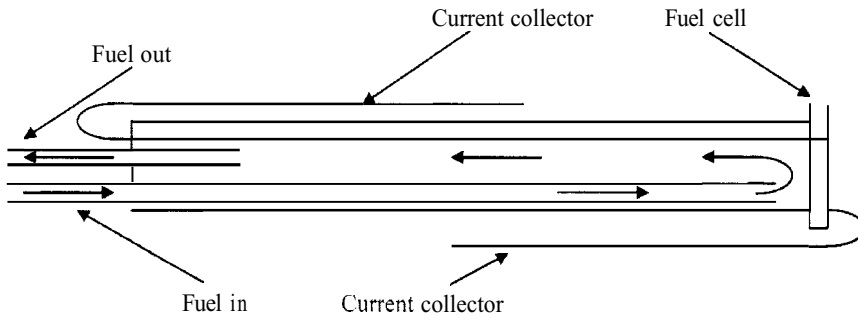


Fig.1. Button SOFC testing rig design

3. RESULTS AND DISCUSSION:

3.1. Evaluation of interfacial anode-electrolyte reactions

Possible interfacial reactions between anode and electrolyte were studied using **XRD** technique. For this purpose LSCM and LSGM powders were mixed in 50:50 ratio and the pellets made out of this mixture were fired for 2 hrs at 1200°C and 5 hrs at **1400°C**. The XRD results obtained for these pellets (Figure 2) do not indicate any interfacial reaction since the corresponding peaks exactly correlate with XRD database. In both case, the major peaks indicating an orthorhombic structure with $a = 5.487$, $b = 5.520$ and $c = 7.752$ Å lattice parameters, which represents lanthanum gallium oxide. The standard lanthanum gallium oxide $\text{LaGaO}_3 / 0.5 (\text{La}_2\text{O}_3, \text{Ga}_2\text{O}_3)$ pattern is shown in Figure 2 to compare with the obtained results. The other peaks about $2\theta=30^\circ$ are related to the anode as well as some other peaks which overlap with those of the standard lanthanum gallium oxide.